

TELKOMNIKA, Vol.16, No.6, December 2018, pp.2570–2577

ISSN: 1693-6930, accredited First Grade by Kemenristekdikti, Decree No: 21/E/KPT/2018

DOI: 10.12928/TELKOMNIKA.v16i6.9968

■ 2570

Loss Quantization of Reflectarray Antenna Based on Organic Substrate Materials

H. I. Malik¹, M. Y. Ismail^{*2}, Sharmiza Adnan³, S. R. Masrol⁴^{1,2,4}Universiti Tun Hussein Onn Malaysia (UTHM), Parit Raja 86400, Batu Pahat, Johor, Malaysia³Forest Research Institute Malaysia (FRIM), Jalan Frim, Kepong, 52109 Kuala Lumpur, Selangor, Malaysia^{*}Corresponding author, e-mail: yusofi@uthm.edu.my

Abstract

This paper presents novel loss quantization of reflectarray elements based on organic substrate materials. Three differently composed substrate materials derived from recycled materials have been characterized for their dielectric properties using a broadband analysis technique. The materials show low dielectric permittivity values of 1.81, 1.62 and 1.84 for X-band frequency range. In order to estimate the reflection loss of for the three substrates a mathematical relation has been established using empirical data generated by computer simulated models. The reliability of the proposed model has been established by simulation and fabrication of unit reflectarray rectangular patch elements on three proposed substrate substrates. A broadband frequency response has been depicted by scattering parameter analysis of unit elements with 10% fractional bandwidth of 312, 340 and 207 MHz for RCP50, RCR75 and RNP50 substrate respectively.

Keywords: reflectarray antenna; paper substrate; reflection loss; scattering parameters

Copyright © 2018 Universitas Ahmad Dahlan. All rights reserved.

1. Introduction

Conventional high gain antenna applications require highly directional and efficient reflectors or phased arrays antennas. Parabolic dish reflector have served the communication industry well in terms of an efficient reflector antenna for long range communication such as space and radar applications [1]. However parabolic dish reflectors are usually bulky and massive in size, moreover they require complex rotatory and movement structures for beam scanning or steering applications. In order to overcome the problems faced by the parabolic dish reflectors a flat printed microstrip reflectarray antenna was introduced that can be used for high gain applications with smaller mass and volume. A reflectarray consists of two main parts an array of elements and a feeding antenna. The phase distribution of elements over the array is strictly controlled in order to focus the main beam of antenna towards a particular direction.

In a reflectarray antenna the printed elements are excited spatially, this eliminates the requirement of using complex and lossy feeding network of microstrip lines, as in phased array antennas. Moreover the low profile and thin structure makes it an attractive choice for small, shrouded places specially spacecraft payloads [2]. The printed elements in reflectarray are distributed as an array over a thin dielectric substrate material. The elements may take different configurations such as variable size patches, parallel or cross dipoles, square or circular rings etc [3-5]. In all the element configurations, the reflection phase of the individual elements is precisely monitored to control the overall array pattern. The reflection phase of an element is dependent upon its dimensions as well as its position on the array.

The evolution of printed circuit board (PCB) technology has made commercial production of flat printed reflectarrays a lot more feasible. On the other hand the production of parabolic dish reflectors requires difficult casting and molding techniques to acquire dish curvature. However reflectarray face challenges in terms of its intrinsic narrow bandwidth and high loss performance. Microstrip reflectarrays are derived from microstrip patch antenna and the patch antenna has an intrinsic bandwidth of just 3-5% only [6]. This drawback of reflectarray has been addressed by using thicker or multi-layer structures but this increases the fabrication complexity of the antenna [7-10]. Along with thicker substrate materials air gaps has also been introduced between the ground plane and the substrate region in order to achieve smoother phase and broadband frequency response [11-13].

Received May 22, 2018; Revised September 13, 2018; Accepted October 4, 2018

The conventional microstrip patch antenna are preferred to be fabricated above commercially available materials such as Rogers Duroid substrates, Taconic RF301 and FR-4 substrate materials. However with the peaking advances in the material and manufacturing industry new and efficient materials are being introduced to achieve enhanced performances. 3D printing has been used for the manufacturing of a dielectric resonator reflectarray based on dielectric resonator element for THz frequencies [14]. The method uses an Objet Eden 350 polymer for 3D printing of the array. In another 3D printed reflectarray utilizes VeroBlue RGD240 material for the printing of an open ended waveguide reflectarray at 60 GHz [15, 16]. The material was later electroplated to achieve an all metallic reflectarray antenna. The use of ceramic ferro-electric materials for phase shifting, beam steering or switching applications has brought a new dimension for reflectarray antennas [17-19]. Barium strontium titanate has been used for the wide phase tuning of reflectarray unit cells. Organic substrate materials based on cellulose material has been reported to be used as substrates for microstrip patch antenna applications [20-23]. The commercially available papers substrate materials are used for frequencies as high as 24 GHz [24]. The concept provides efficient low cost antenna electronics along with fabrication ease.

This research proposes three novel organic substrate materials derived from paper substrate for microstrip reflectarray antenna. The composition of the paper substrate is controlled in order to achieve diverse material properties. The proposed material has been characterized thoroughly using a dielectric probe method. This paper also presents the reflection loss quantization of rectangular patch elements on the three proposed substrates. A mathematical model has been derived by relating the reflection loss with substrate height and the resonant frequency. The paper also presents the fabrication and measurement of rectangular patch elements on proposed substrate materials.

2. Organic Substrate Materials

2.1. Material Preparation

A paper is usually made up of a combination of particle suspension bounded by a fibrous component. The fibrous component bonds the suspended particles and provides strength and stress properties to the paper. The proposed substrate has been derived from recycled material such as copier paper, carton paper and the newspaper. Banana fiber has been used as binding fiber to add strength properties to the paper material. The three proposed paper substrates along with their composition and used acronyms are presented below:

- a. Newspaper (50%) + Banana Pulp (50%) ; RNP50
- b. Carton box (75%) + Banana pulp (25%) ; RCR75
- c. Copier Paper (50%) + Banana Pulp (50%) ; RCP50

The paper substrate materials were processed to achieve uniform sheets of paper. The sheets were then glued together to achieve thick substrates samples suitable for microstrip patch antenna applications. The samples were passed through various stages of pressing, rolling and heating to remove the moisture content of glue. This was done in order to minimize the effect of moisture on the dielectric material properties.

2.2. Dielectric Material Characterization

The proposed papers substrate materials were characterized for their dielectric material properties. The method used for characterization was based on dielectric probe method; a broadband characterization technique. The setup used for characterization is presented in Figure 1. It consists of a Speag Dielectric Assessment Kit (DAK) 3.5 mm probe. The probe provides an analysis range of 0.2–20 GHz. The system uses a vector network analyzer and a software platform installed at the PC. The probe is controlled remotely by the PC via VNA. A 14 GHz Rodhe & Schwarz network analyzer has been used for this purpose. The analysis of the proposed materials was done for X-band frequency range. Figure 1 (a) shows the proposed substrate materials with commercially available substrates such as FR-4 and Rogers Duroid 5880. The material characterization setup shows the dielectric probe used for the analysis as shown in Figure 1 (b). The setup was calibrated precisely using water as a load material due to universal properties of water. The dielectric material characterization results are presented in Figure 2 and Figure 3.

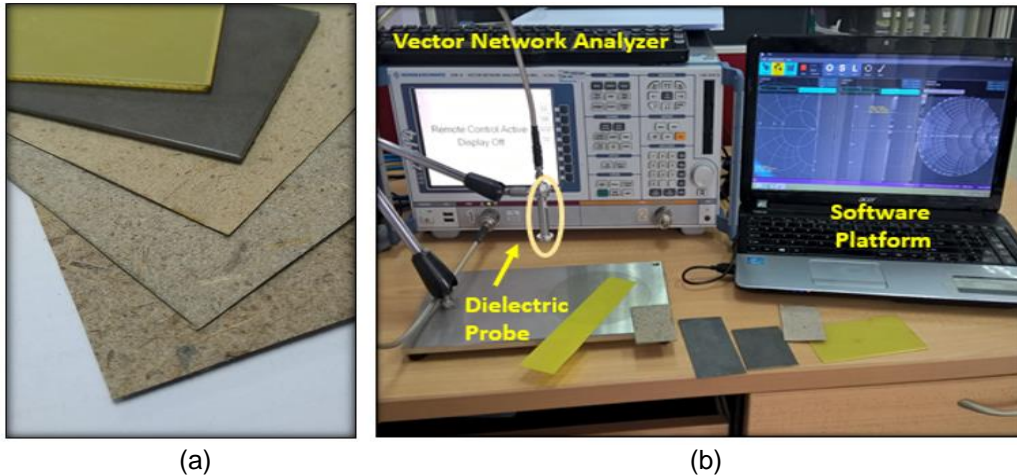


Figure 1. Dielectric material characterization (a) proposed dielectric materials (b) material characterization setup

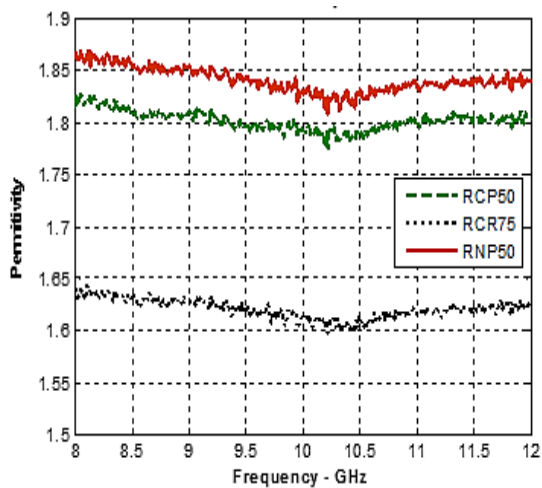


Figure 2. Relative permittivity results for three proposed substrates

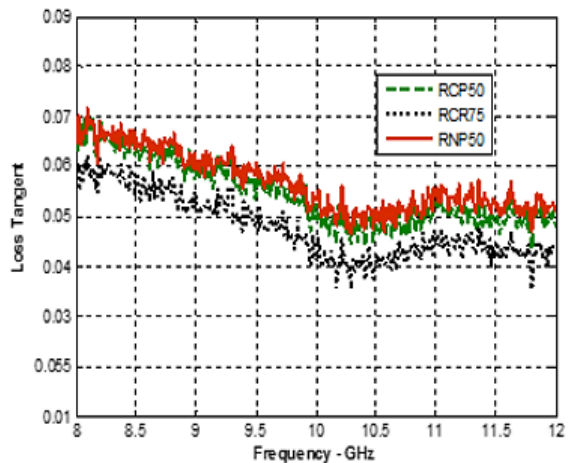


Figure 3. Loss tangent results for material characterization of paper substrate materials

The results presented in Figure 2 shows the relative permittivity for the three proposed substrates. The results depict that there is a minor variation of permittivity over the entire X-band. The findings from Figure 2 and Figure 3 are tabulated in Table 1.

Table 1. Dielectric Material Characterization

Substrate	ϵ_r	$\tan\delta$
RCP50	1.81	0.053
RCR75	1.63	0.046
RNP50	1.84	0.057

The presented values are the mean values over X-band frequency range. The presented results show that the substrate materials RCP50, RCR75 and RNP50 substrate shows dielectric permittivity of 1.81, 1.63 and 1.84 along with loss tangents of 0.053, 0.046 and 0.057 respectively.

3. Reflection Loss Quantization

This section provides the mathematical modeling for the reflection loss estimation of rectangular patch element on proposed substrate material. Full-wave computer simulation model based on finite integral method (FIM) was used to model a rectangular patch element on dielectric slab of proposed substrates. The simulation model utilizes the concept of closed boundary conditions with conductive walls and normal incidence of E-field to realize an infinite array of elements. The simulated model with applied boundary conditions is presented in Figure 4, where the electric and magnetic wall are also labelled. The incident E-field operates with TE₁₀ mode of operation.

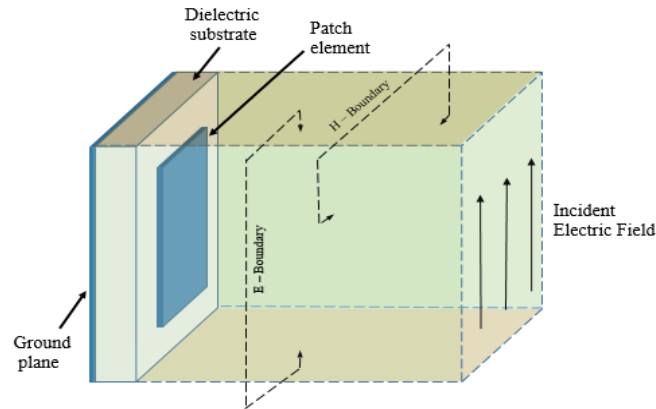


Figure 4. Unit reflectarray element with closed boundary conditions and normal E- field incidence

Mathematical modelling was done by taking in to consideration three parameters of unit reflectarray design while keeping the others as constant. Different parameters was made constant to simplify the fitting process. The variable taken under consideration were substrate height, resonant frequency and the reflection loss. Other parameters such as the dielectric properties, patch antenna dimensions, boundary conditions and incidence angle were all kept constant. The empirical data was generated by sweeping the substrate heights between the ranges of 0.6–3.0 mm for all the three substrates. During the data generation special consideration was taken in terms of reflection phase of the element so that the reflection phase does not get corrupted. The range 0.6–3.0 was selected also to keep the resonant frequency range within the limits of X-band (8–12 GHz).

Linear polynomial fitting technique based on linear regression was utilized to fit a polynomial to the empirical data. The empirical data was utilized to generate linear polynomials that best describe the relation between the reflection loss, substrate height and the resonant frequency. The fitted polynomials are presented below:

$$RL_{RCP50} = 2715 - 794 h - 243.8 f_r + 47.13 h^2 + 52 h f_r \quad (1)$$

$$RL_{RCR75} = -159 + 574.9 h + 139.8 f_r - 36.2 h^2 - 39.25 h f_r \quad (2)$$

$$RL_{RNP50} = 6502 - 6906 h - 575.8 f_r + 2210 h^2 + 569.3 h f_r - 125.7 h^3 - 154.4 h^2 f_r \quad (3)$$

The above equations relate the reflection loss with the substrate height and the resonant frequency of a rectangular unit reflectarray patch element where RL represents the reflection loss, h represents the substrate height and f_r represents the resonant frequency. The above solution is only applicable to X-band frequency range. In order to validate the proposed model for the estimation, a comparison was drawn between the empirical data used for fitting and the actual fit. Figure 5 presents the comparison for validation of model. In the figure

the solid lines represent the actual simulated data from the software while the dotted and dashed lines represent the different types of fitting calculated from the (1-3).

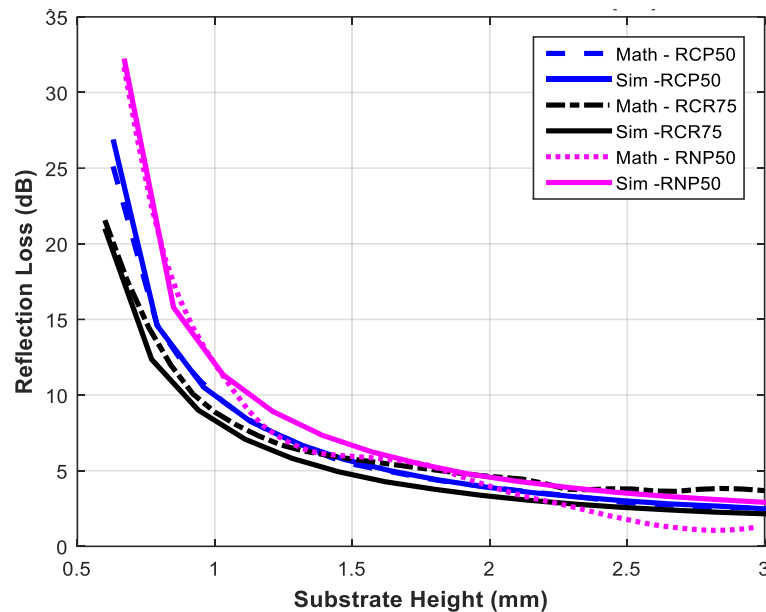


Figure 5. Comparison between the simulated reflection loss and the modelled loss using mathematical relation

The results of validation show that there is a close agreement between the empirical data and the actual mathematical fits. The presented results in Figure 5 show that for RNP50 substrate material maximum loss trend is being followed to -32 dB where the modelled curve also follows the actual curve very closely however it can be seen deviating from the actual loss in the range between 2-3 mm. The curve for RCP50 substrate material shows that the simulated data gives the maximum loss of -26.3 dB followed by the reflection loss calculated by (1) i.e. 25.1 dB. The difference between the data and the mathematical model decreases as the substrate height is increased. The comparison provided for RCR75 substrate material curve is also presented in Figure 5 with both simulated data and the loss calculated using (2). The results show that simulated and calculated losses are 21.01 and 21.56 dB respectively. The reflection loss shows a gradually decreasing trend as the substrate height is increased. Thus the presented results show that the fitted model using empirical data follow closely with the empirical data with an average discrepancy below 10% for all the substrate materials.

4. Fabrication and Measurements

In order to realize the reflectarray antenna based on rectangular patch elements, unit elements were fabricated on three proposed substrate materials. The fabrication process used was based on manual cutting of adhesive copper tape. Adhesive copper tape was preferred over conductive printed ink based on silver nano-particles because copper tape provides conductivity of bulk copper that reduces the conductor losses at high frequencies. The silver nano-particle ink also requires sintering process at high temperatures for proper deposition that might affect the cellulose based paper substrate. The proposed substrate material is also not robust enough to withstand the CNC milling or wet chemical etching process. Thus manual cutting was the most suitable process to be used for fabrication. Rectangular patch elements fabricated above proposed substrate are presented in Figure 6.

The elements fabricated were measured for the dimensions after the fabrication. The simulation results were then updated to the actual fabricated dimension to eliminate any errors. The fabricated elements were measured for the scattering parameters using an X-band

waveguide simulating based on the technique proposed in [25]. A Rodhe and Schwarz 14 GHz Vector Network Analyzer was used for measurements. The complete measurement setup is shown in Figure 7. The elements are placed inside the waveguide aperture shown in Figure 7 (a) and the reflection loss and reflection phase response of the elements is measured. Figure 7 (b) shows the complete measurement setup.

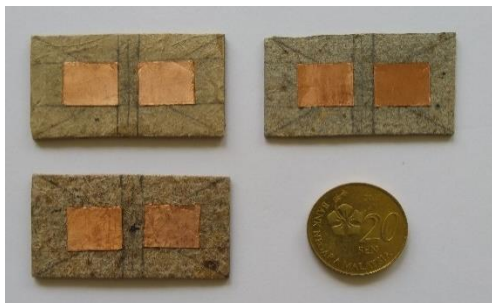


Figure 6. Fabricated unit reflectarray elements on proposed organic substrate materials

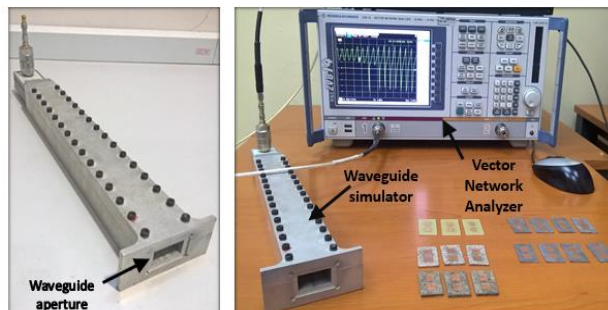


Figure 7. Scattering parameter measurements
(a) waveguide simulator
(b) complete measurement setup

The scattering parameter results for all the three proposed substrate are presented in Figure 8 and Figure 9. The reflection loss curves show a close agreement between the measured and simulated results. The dotted lines represent the measured results. The ripples present in the measured results are due to non-ideal nature of waveguide simulator. Figure 8 shows the results for reflection loss curves. It can be seen that the RNP50 substrate material shows the maximum reflection loss and a minimum reflection loss is shown by RCR75 substrate material. The reflection phase curves are presented in Figure 9. The results show gradual change in slope curves from maximum to minimum with maximum gradient at the resonance point. This is due pure resistive behavior at the resonance. The finding from Figure 8 and Figure 9 are tabulated in Table 2.

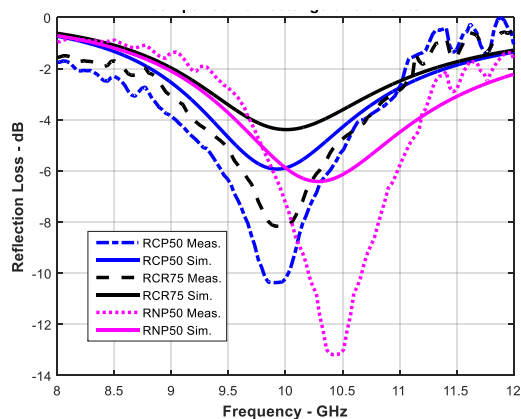


Figure 8. Comparison between measured and simulated reflection loss for rectangular patch elements

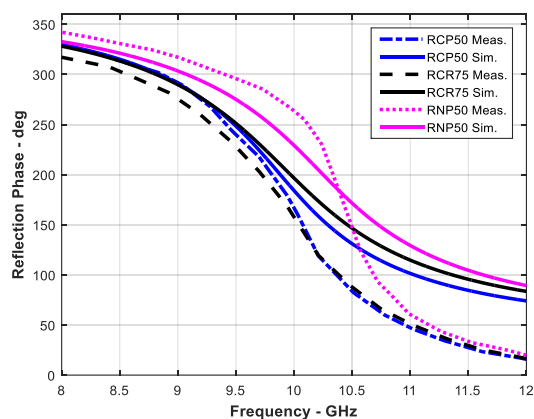


Figure 9. Reflection phase curves for rectangular patch elements on unit reflectarray elements

The summary of the results presented in Table 2 show that the rectangular patch elements show resonances at 9.94, 9.95 and 10.42 GHz for RCP50, RCR75 and RNP50 substrate materials respectively. The reflection loss for measured curves is -10.36, -8.14

and -13.19 dB for RCP50, RCR75 and RNP50 substrate materials respectively. A 10 % bandwidth was also defined by moving 10% above the maximum loss level on the reflection loss curve. The results show the maximum fractional bandwidth of 340 MHz for RCR75 substrate materials followed by 312 and 207 MHz for RCP50 and RNP50 substrate materials respectively. The calculated phase range for the element is also presented with a maximum phase range of 319° shown by RNP50 substrate material and a minimum phase range of 301° shown by RCR75 substrate material with RCP50 substrate materials showing an intermediate phase range of 308°. In order to establish a relation between the reflection phase and the bandwidth of the reflectarray element a metric Figure of Merit (FOM) has been defined. The FOM shows the gradient of the phase curve with respect to changing frequency. The FOM calculated for all the phase curves show that the maximum FOM of 0.28 °/MHz is shown by RNP50 substrate element while a minimum phase gradient is shown by 0.14 °/MHz. The RCP50 substrate element shows a gradient of 0.19 °/MHz.

Table 2. Scattering Parameter Results for Rectangular Patch Element on Proposed Substrate Material

Substrate (height - mm)		fr (GHz)	RL (dB)	Δf (MHz) 10%	$\Delta\Phi$ (deg)	FOM (°/MHz)
RCP50	Sim.	9.92	-5.92	465	254	0.13
	Mea.	9.94	-10.36	312	308	0.19
RCR75	Sim.	9.98	-4.38	682	243	0.10
	Mea.	9.95	-8.16	340	301	0.14
RNP50	Sim.	10.46	-6.41	356	275	0.12
	Mea.	10.42	-13.19	207	319	0.28

The presented results for the rectangular patch element on three proposed substrates show good agreement between the simulated and the measured results. The presented organic substrate materials will provide an eco-friendly solution for the future electronic industry. The microstrip reflectarray antenna fabricated using proposed substrates also shows a broadband frequency response compared to conventional substrates that will address the narrow bandwidth limitation.

5. Conclusion

Organic substrate material derived from recycled materials has been presented for microstrip reflectarray antenna. The proposed substrate materials were thoroughly characterized for the dielectric properties. The characterization results shows low dielectric permittivities of 1.81, 1.62 and 1.84 for RCP50, RCR75 and RNP50 substrate materials. A mathematical model has been defined using empirical data generated from computer simulated model. Linear polynomial fitting have been used to establish a mathematical relation between reflection loss, resonant frequency and the substrate height. The developed mathematical relation has been validated for the reflection loss values and a close agreement has been established. In order to realize the simulated models, unit reflectarray elements were fabricated on all the three substrate materials. The scattering parameter results show broadband frequency responses to solve the narrow bandwidth limitation of microstrip reflectarray technology.

References

- [1] Encinar J A, Tienda C, Barba M, Carrasco E, Arrebola M. *Analysis, Design and Prototyping of Reflectarray Antennas for Space Applications*. Loughborough Antennas and Propagation Conference (LAPC). 2013: 1–5.
- [2] Encinar J A. "Printed Reflectarray Antennas for Space Applications," in *Space Antenna Handbook*, 2012: 385-434.
- [3] Tienda C, Arrebola M, Encinar J A, Toso G. Analysis of a Dual-Reflectarray Antenna. *IET Microwaves, Antennas Propagation*. 2011; 5(13): 1636–1645.
- [4] Yoon J H, Yoon Y J, Lee W, So J. Broadband Microstrip Reflectarray with Five Parallel Dipole

- Elements. *IEEE Antennas and Wireless Propagation Letters*. 2015; 14: 1109–1112.
- [5] Encinar J A, et al. *Dual-Polarization Reflectarray in Ku-band Based on Two Layers of Dipole-Arrays for a Transmit-Receive Satellite Antenna with South American Coverage*. 2017 11th European Conference Antennas Propagation. 2017: 80–83.
- [6] Kumar G, Ray K P. *Broadband Microstrip Antennas*. Artech House. 2003.
- [7] Encinar J A, Zornoza J A. Three-Layer Printed Reflectarrays for Contoured Beam Space Applications. *IEEE Transactions Antennas Propagation*. 2004; 52(5): 1138–1148.
- [8] Duan X C, Xia Y X, Zhou Y, Li B, Liu Y, Lv X. *A Novel Double-Layered Dielectric Reflectarray*. 2016 IEEE 9th UK-Europe-China Workshop on Millimetre Waves and Terahertz Technologies (UCMMT). 2016: 94–95.
- [9] Smith T, Gothelf U, Kim O S, Breinbjerg O. An FSS-backed 20/30 GHz Circularly Polarized Reflectarray for a Shared Aperture L- and Ka-band Satellite Communication Antenna. *IEEE Transactions Antennas Propagation*. 2014.
- [10] Samsuri N H S N A, Rahim M K A, Seman F C, Inam M. Compact Meander Line Telemetry Antenna for Implantable Pacemaker Applications. *Indonesian Journal of Electrical Engineering and Computer Science*. 2018; 10(3): 883–889.
- [11] Deng R, Xu S, Yang F, Li M. Single-layer Dual-band Reflectarray Antennas with Wide Frequency Ratios and High Aperture Efficiencies Using Phoenix Elements. *IEEE Transactions Antennas Propagation*. 2017; 65(2): 612–622.
- [12] Yoon J H, Yoon Y J, Lee W, So J. Square Ring Element Reflectarrays with Improved Radiation Characteristics by Reducing Reflection Phase Sensitivity. *IEEE Transactions Antennas Propagation*. 2015; 63 (2): 814–818.
- [13] Han C, Huang J, Chang K. A High Efficiency Offset-Fed X/Ka-Dual-Band Reflectarray Using Thin Membranes. *IEEE Transactions Antennas Propagation*. 2005; 53(9): 2792–2798.
- [14] Nayeri P, et al. 3D Printed Dielectric Reflectarrays: Low-cost High-gain Antennas at Sub-millimeter Waves. *IEEE Transactions Antennas Propagation*. 2014; 62(4): 2000–2008.
- [15] Chen B J, Yi H, Ng K B, Qu S W, Chan C. H. *3D Printed Reflectarray Antenna at 60 GHz*. International Symposium on Antennas and Propagation (ISAP). 2016: 92–93.
- [16] Feiz N, Mohajeri F, Ghaznavi A. Optimized Microstrip Antennas with Metamaterial Superstrates using Particle Swarm Optimization. *Bulletin of Electrical Engineering and Informatics*. 2013; 2(2): 123–131.
- [17] Modelski J W, Yashchyshyn Y. Microwave Ferroelectric and Reconfigurable Antennas. *IEEE MTT-S Int. Microw. Work. Ser. Millim. Wave Wirel. Technol. Appl.* 2012: 1–2.
- [18] Romanofsky R. R. Advances in Scanning Reflectarray Antennas Based on Ferroelectric Thin-Film Phase Shifters for Deep-space Communications. *Proceedings of the IEEE*. 2007; 95(10): 1968–1975.
- [19] Malallah Y, et al. *Tunable Microwave Filters Using Nanoparticles and Thin Films of Ferroic Materials*. 16th Mediterranean Microwave Symposium (MMS). 2016: 2–5.
- [20] Leng T, Huang X, Chang K, Chen J, Abdalla M A, Hu Z. Graphene Nanoflakes Printed Flexible Meandered-Line Dipole Antenna on Paper Substrate for Low-Cost RFID and Sensing Applications. *IEEE Antennas and Wireless Propagation Letters*. 2016; 15: 1565–1568.
- [21] Cook B S, Shamim A. Utilizing Wideband AMC Structures for High-Gain Inkjet-Printed Antennas on Lossy Paper Substrate. *IEEE Antennas and Wireless Propagation Letters*. 2013; 12: 76–79.
- [22] Kanagasabai M, Kizhekke Pakkathillam J. Performance Evaluation of a Dual Band Paper Substrate Wireless Sensor Networks Antenna over Curvilinear Surfaces. *IET Microwaves, Antennas Propagation*, 2015.
- [23] Bala R, Marwaha A, Marwaha S. Material Modeling Approach for Graphene Antenna Design. *Indonesian Journal of Electrical Engineering and Computer Science*. 2015; 16(3): 480–487.
- [24] Mezzanotte P et al. 24-GHz Patch Antenna Array on Cellulose-Based Materials for Green Wireless Internet Applications. *IET Science, Measurement, and Technoogy*. 2014; 8(6): 342–349.
- [25] Stockmann J, Hodges R. *The Use of Waveguide Simulators to Measure the Resonant Frequency of Ku-band Microstrip Arrays*. IEEE Antennas and Propagation Society, AP-S International Symposium (Digest). 2005; 1: 417–420.